

## PLANT PROTEIN-MEDIATED SIZE-CONTROLLED SYNTHESIS OF MAGNETITE NANOPARTICLES - STUDIES ON OPTICAL PROPERTIES

Amlan Kumar Das<sup>1\*</sup>, Vijendra Singh Solanki<sup>2\*</sup>, Apoorva Fanan<sup>1</sup>, Neha Agarwal<sup>3</sup> and Virendra Kumar Yadav<sup>4</sup>

<sup>1</sup>Department of Chemistry, School of Liberal Arts and Sciences, (SLAS), Mody University of Science and Technology, Lakshmangarh, Sikar - 332311, Rajasthan, India

<sup>2</sup>Department of Chemistry, ISR, IPS Academy, Indore – 452012, Madhya Pradesh, India

<sup>3</sup>Department of Chemistry, Navyug Kanya Mahavidyalaya, University of Lucknow, India

<sup>4</sup>Department of Life Sciences, Hemchandracharya North Gujarat University, Patan, India

(Received May 12, 2023; Revised October 23, 2023; Accepted November 18, 2023)

**ABSTRACT.** In today's scenario nanotechnology has great importance in all scientific and non-scientific sectors. In this study, we have synthesized magnetite nanoparticles coated by the proteins available in the *Datura* leaf extract through a green and eco-friendly method. From the resulting spectrum obtained on Fe<sub>3</sub>O<sub>4</sub> for different volumes of leaf extract of *Datura* leaf, the surface plasmon resonance seems to be varying with the volume of capping agent. The data shows that as the volume of capping agent increases the SPR value is shifted to red-end. The E<sub>g</sub> values increase with the increasing volume of capping agents. The evaluated band gap (E<sub>g</sub>) values are close to semiconductors (0-3 eV). The values indicate that the formed Fe<sub>3</sub>O<sub>4</sub> nanoparticles are marginally semiconducting. The E<sub>g</sub> values are found to be dependent upon the volume of the capping agent. The properties of nano-sized semiconductor particles depend on particle size. Here, the absorption peaks (λ<sub>max</sub>) are consistently increased giving rise to red-shift. The value of surface plasmon resonance shift confirmed that particle size is decreased.

**KEY WORDS:** Green synthesis, Magnetite nanoparticles (MNPs), Leaf extract, Band gap, Optical properties, Surface plasmon resonance

### INTRODUCTION

In these days, green synthesis and applications of nanomaterials in different sectors such as agriculture, medical, textiles, manufacturing industries, biomedical and pharmaceutical, waste water treatment, sectors have been appreciated very much [1-3].

The advantages of green synthesis over chemical and physical synthesis are low cost, low energy, eco-friendliness and simple technique. Due to the unique physical and chemical properties of properties of Fe<sub>3</sub>O<sub>4</sub> NPs such as biodegradability, magnetic, biocompatibility and heat mediated properties; these are used in medical field in treatment of various diseases such as pulmonary diseases [4-6] like cancer [7-10], and tissue engineering [11]. Magnetite NPs also work as effective photocatalysts in the waste-water treatment since their magnetic properties favor the effective oxidation of organic pollutants released by various chemical, pharmaceuticals, textile and leather industries [12-14]. In the year 2021, Altaf *et al.* successfully degraded the antibiotic levofloxacin from the aqueous solution by green synthesized MNPs (Fe<sub>3</sub>O<sub>4</sub>) and concluded that it can be reused up to four cycles [15]. Xiahong Shi *et al.* in 2022, removed toxic and potential pollutant microplastics from the water bodies by MNPs [16].

The conventional chemical synthesis requires high energy, toxic materials, high cost and no atom economy, so in this study, the magnetite nanoparticles (MNPs) were synthesized by using the *Datura* leaf extract and metallic solutions through green and ecofriendly approach. Here, MNPs was synthesized by *Datura* leaf extract by reduction of Fe<sup>2+</sup> and Fe<sup>3+</sup> ions to Fe<sub>3</sub>O<sub>4</sub> NPs from ferrous and ferric chloride solution within few min of start of reaction at 80 °C. The average size of magnetite nanoparticles can be controlled by varying the volume of the leaf extract. Plant

\*Corresponding author. E-mail: [amlan.snigdha72@gmail.com](mailto:amlan.snigdha72@gmail.com); [vijendrasingh0018@gmail.com](mailto:vijendrasingh0018@gmail.com)  
This work is licensed under the Creative Commons Attribution 4.0 International License

protein coated core-shell structure of magnetic nanoparticles seems to have colloidal stability and magnetic stability as confirmed by SQUID study [17] which confirms that the protein-coated nano bio-hybrid magnetite shows super-paramagnetic behavior.

The band gap of the magnetic nano particles has been increased with the decrease in particle size. The surface plasmon resonance increases with the increase in volume of capping agent. The data shows that as the volume of capping agent increases the surface plasmon resonance value is shifted to red end. This newly surface-modified synthesized magnetite particle can be used as semiconductors.

## EXPERIMENTAL

### *Collection and preparation of Datura leaf extract*

About 500 g of Datura leaf were collected from the Mody University of Science and Technology (MUST), Rajasthan, India, and washed with distilled water to remove stuck dust and other particles and then kept it at room temperature for 14 days to remove moisture present in the leaves. Then dry leaves were ground in a mortar into small pieces taken 40 g dried powder and boiled in 500 mL RB flask, by adding of 300 mL doubled distilled water and methyl alcohol for 1 h at 60 °C on a magnetic stirrer. The extract was filtered through Whatman filter paper – 42 and kept in a refrigerator. The filtrate was used in the synthesis of magnetic nanoparticles [18].

### *Synthesis of magnetite nanoparticles ( $Fe_3O_4$ )*

The MNPs were synthesized by green route through Datura leaf extract. 10 mL of 0.05 M  $FeCl_2 \cdot 4H_2O$  and 1 mL of 0.1 M  $FeCl_3 \cdot 6H_2O$  (2:1) were added to the 100 mL of leaf extract with NaOH in 250 mL beaker and heated at 80 °C under mild stirring for 1 h. The dark red color precipitates were obtained which indicates the synthesis of MNPs. The dark red color MNPs are washed by re-dispersion in distilled water. The mixture was kept in the refrigerator at low temperature for rapid precipitation. The gradual change of colour of the nanoparticle formation has been shown in Figure 1.

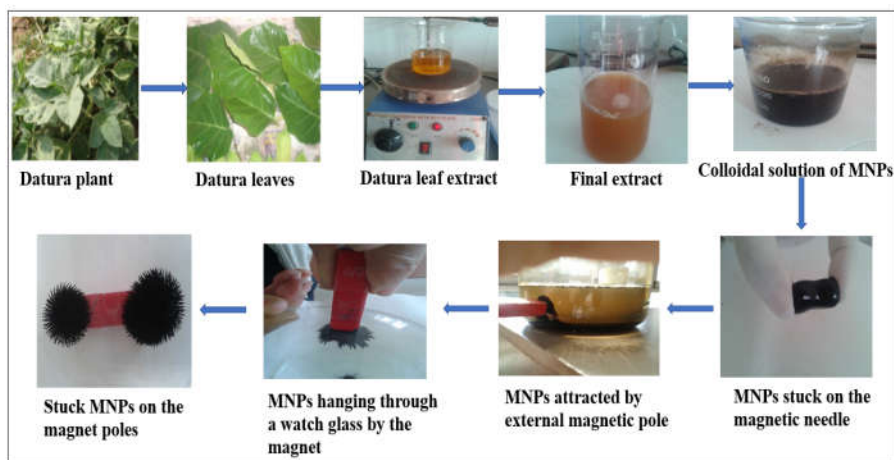
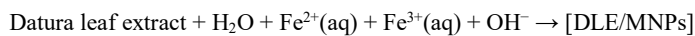


Figure 1. Synthesis of MNPs by Datura leaf extract.



The reduction of  $\text{Fe}^{3+}$  to  $\text{Fe}^{2+}$  is due to the presence of various organic compounds such as phenols, protein, cardiac glycosides, flavonoids etc. in Datura leaf extract [19].

The MNPs colloidal solution was dried and characterized by the FTIR technique. The same procedure was applied for 10, 20 and 30 mL Datura leaf extract which is shown in Figure 2.

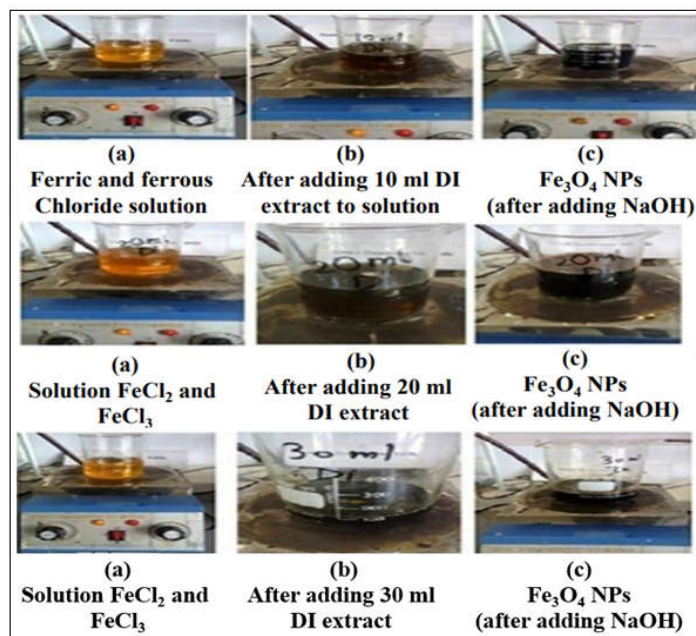


Figure 2. Preparation of nanoparticles by using different volumes of Datura leaf extract (10, 20, 30 mL).

Figure 3 shows the dark red color of the  $\text{Fe}^{3+}/\text{Fe}^{2+}$  solution after adding Datura leaf extract and NaOH at 80 °C.

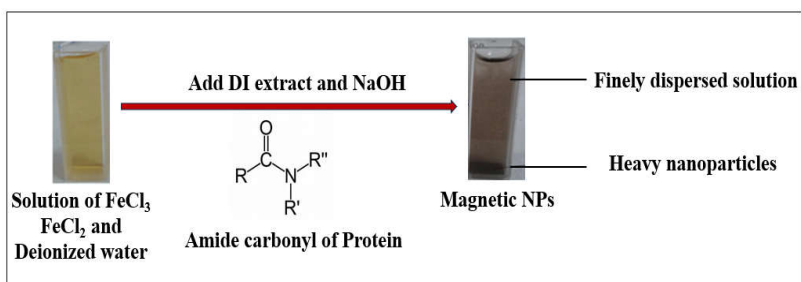


Figure 3. Photograph of synthesized  $\text{Fe}_3\text{O}_4$ -NPs in Datura leaf extract.

## RESULTS AND DISCUSSION

The nanosized Fe<sub>3</sub>O<sub>4</sub> was characterized by different techniques such as FTIR, TGA, XRD, TEM, UV-Vis detailed studies have been reported in the published paper [18]. The coated protein layers on the nanosized Fe<sub>3</sub>O<sub>4</sub> particles were confirmed by Fourier-transform infrared spectroscopy (FT-IR) and thermogravimetric analysis (TGA), nature of the crystalline particle and particle size was determined by X-ray diffraction (XRD) and Transmission electron microscopy (TEM), respectively.

### *Size control and influence of particle size on the optical properties*

Figure 4 shows the UV-Vis spectra of Fe<sub>3</sub>O<sub>4</sub> for different volumes of freshly prepared Datura leaf extract. The UV-Visible spectral data were observed at 390, 370, 355 and 345 nm; where the absorbance value is minimum for 5, 10, 20 and 30 mL of extract volume, respectively.

The surface plasmon resonance seems to be varying with the volume of the capping agent which has been recorded in Table 1. The data shows that as the volume of capping agent increases the SPR value is shifted to red end.

Table 1. Capping agent concentration and SPR.

Different volumes of capping agent	SPR ( $\lambda_{max}$ )
5 mL of extract	218
10 mL of extract	228
20 mL of extract	234
30 mL of extract	249

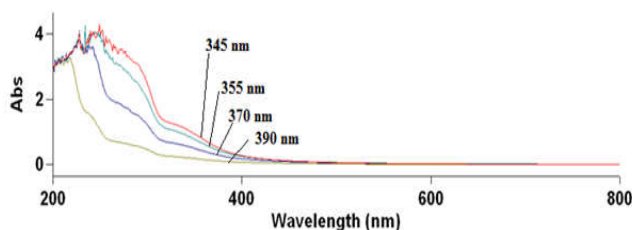


Figure 4. UV/Vis absorption measurements of Fe<sub>3</sub>O<sub>4</sub> nanoparticles for different concentrations of Datura leaf extract - (X), where X = different concentrations of Datura leaf extract, X = 5 mL (light green), 10 mL (Dark blue), 20 mL (light blue), 30 mL (red).

### *Band gap calculation*

The optical band gap of the synthesized nanomaterials was calculated by the following equation: Band gap energy ( $E_g$ ) =  $h*c/\lambda$  [17, 20]. The calculated values of the band gap of each sample with different volumes of capping agents have been presented in Table 2.

The  $E_g$  values increase with increasing volume of capping agent. The evaluated  $E_g$  values are close to semiconductors (0-3 eV). The values indicate that the formed Fe<sub>3</sub>O<sub>4</sub> nanoparticles are marginally semiconducting. The  $E_g$  values are found to dependent upon volume of the capping agent [21].

Table 2. Band gap energy values of Fe<sub>3</sub>O<sub>4</sub> obtained for different volumes of capping agent.

Different conc. of capping agent	$\lambda$ (cut off)	$E_g$ (J)	$E_g$ (eV)
5 mL	390 nm	$5.09 \times 10^{-19}$	3.18
10 mL	370 nm	$5.37 \times 10^{-19}$	3.35
20 mL	355 nm	$5.59 \times 10^{-19}$	3.499
30 mL	345 nm	$5.76 \times 10^{-19}$	3.6

#### Relation between band gap and particle size

The relation between particle size and band gap has been established with the help of UV-Vis. The properties of nano-sized semiconductor particles depend on particle size. The spacing of the levels and the bandgap increases with decreasing particle size. Here, the absorption peaks ( $\lambda_{\max}$ ) are consistently increasing giving rise to red shift which indicates that the particle size must be decreasing [22].

According to the reference, the average particle size is decreased by increasing the concentration of the surface-active agent. In the absorption spectrum, peak is obtained in UV region and shifts towards higher wavelength ( $\lambda$ ) by increasing the capping agent volume. This indicates an increase in the effective band gap [17]. The variation of particle size, band gap and absorption peaks (SPR) with the volume of capping agent have been mentioned in Table 3.

Table 3. Different volumes of capping agent and particle size.

Different volume of capping agent	Absorption peaks ( $\lambda_{\max}$ )	$E_g = hc/\lambda$	Particle size
5 mL of extract	218	3.18	Must decrease
10 mL of extract	228	3.35	
20 mL of extract	234	3.50	
30 mL of extract	249	3.6	

From Table 3, it can be understood that as the Datura leaf extract volume increases absorption peak ( $\lambda_{\max}$ ) also increases, as a result band gap increases. Conceptually it is seen that particle size decreases as the band gap of the sample increases. Since the absorption peak is consistently increasing, it shows the red shift and its band gap increases [23].

#### Relation between SPR and particle size

Surface plasmon energy is affected by the dimensions of nanoparticles. With the decrease in size of nanoparticles the surface plasmon resonance moves toward the red end of the spectrum. The rate of scattering of the conduction electrons on the nanoparticle surface increases with the decrease of the size of nanoparticles, which results in a nonlinear red shift of the SPR.

The decrease in the size of nanoparticle with increase of the bandwidth is because of the scattering of the conduction band electrons [24]. The corresponding UV-Vis extinction spectra of the four mentioned samples for 5, 10, 20 and 30 mL Datura leaf extract can be found in Figure 4.

From Table 1, we can see the LSPR (localised surface plasmon resonance) extinction maximum,  $\lambda_{\max}$  (228 nm) of the 10 mL DI extract-MNPs sample is red-shifted by 10 nm from the  $\lambda_{\max}$  (218 nm) of the 5 mL DI extract - MNPs sample. The  $\lambda_{\max}$  (234 nm) of 20 mL Datura leaf extract - MNPs sample is red-shifted by 6 nm from the  $\lambda_{\max}$  (228) of the 10 mL Datura leaf extract-MNPs sample.

Similarly,  $\lambda_{\max}$  (249 nm) of 30 mL Datura leaf extract - Fe<sub>3</sub>O<sub>4</sub> nanoparticle sample is shifted towards red end by 15 nm from the  $\lambda_{\max}$  (234 nm) of the 20 mL Datura leaf extract - Fe<sub>3</sub>O<sub>4</sub>

nanoparticle sample. This red-shift is due to a decrease in band gap can be attributed to the thick adsorbate layer on the MNP's local dielectric environment [25].

### CONCLUSION

The MNPs were synthesized by reduction of FeCl<sub>3</sub> with Datura leaf extract containing phenolic and other organic compounds. As a result, a core-shell structure is formed. As a particle goes from bulk to nano and creates new surfaces. This increase in surface is not thermodynamically favorable. The surfaces combine and agglomerate to each other. To prevent agglomeration and ensure magnetic stabilization the surface modification must be done which makes NPs less toxic, biodegradable and biocompatible. It can be understood that as the DI extract volume increases absorption peak ( $\lambda_{\text{max}}$ ) also increases, as a result band gap increases. The advantages of green synthesis over chemical and physical synthesis are low cost, low energy, eco-friendliness and simple technique. Synthesized Nano materials have applications in nanobiotechnology, biomedicine, diagnosis, and drug delivery systems.

### ACKNOWLEDGMENTS

Authors are thankful to Mody University of Science and Technology for providing financial support as seed money (Ref. No. SM/2022-23/001) and ISR, IPS Academy for providing laboratory support.

### REFERENCES

1. Dogiparthi, L.K.; Sana S.S.; Shaik, S.Z.; Kalvapalli, M.R.; Kurupati, G.; Kumar, G.S.; Gangadhar, L. Phytochemical mediated synthesis of silver nanoparticles and their antibacterial activity. *SN Appl. Sci.* **2021**, *3*, 631.
2. Pradeep, M.; Kruszka, D.; Kachlicki, P.; Mondal, D.; Frankli, G. Uncovering the phytochemical basis and the mechanism of plant extract-mediated eco-friendly synthesis of silver nanoparticles using ultra-performance liquid chromatography coupled with a photodiode array and high-resolution mass spectrometry. *ACS Sustainable Chem. Eng.* **2022**, *10*, 562-571.
3. Victor Alfredo Reyes, V.; Jesús Isaías De León, R.; Esteban Hernandez, G.; Sergio Perez, S.; Lilia Angelica Hurtado, A.; Bertha Landeros, S. Synthesis and characterization of magnetite nanoparticles for photocatalysis of nitrobenzene. *J. Saudi Chem. Soc.* **2020**, *24*, 223-235.
4. Shahwan, T.; Abu Sirriah, S.; Nairat, M. Green synthesis of iron nanoparticles and their application as a Fenton-like catalyst for the degradation of aqueous cationic and anionic dyes. *Chem. Eng. J.* **2011**, *172*, 258-266.
5. Das, A.K.; Fanan, A.; Ali, D.; Solanki, V.S.; Pare, B.; Almutairi, B.O.; Agrawal, N.; Yadav, N.; Pareek, V.; Yadav, V.K. Green synthesis of unsaturated fatty acid mediated magnetite nanoparticles and their structural and magnetic studies. *Magnetochemistry* **2022**, *8*, 174.
6. Shireen, I.H.; Sewgil, S.A.; Parween, M.A.; Kwestan, H.S. Biogenic synthesis of ferrous(III) oxide and Fe<sub>3</sub>O<sub>4</sub>/SiO<sub>2</sub> using *Chlorella sp.* and its adsorption properties of water contaminated with copper(II) ions. *Bull. Chem. Soc. Ethiop.* **2022**, *36*, 585-596.
7. El-Sherbiny, I.M.; Elbaz, N.M.; Sedki, M.; Elgammal, A.; Yacoub, M.H. Magnetic nanoparticles-based drug and gene delivery systems for the treatment of pulmonary diseases. *Nanomedicine (London, England)* **2017**, *12*, 387-402.
8. Song, Q.; Javid, A.; Zhang, G.; Li, Y. Applications of magnetite nanoparticles in cancer immunotherapies: Present hallmarks and future perspectives. *Front. Immunol.* **2021**, *4*, 701485.

9. Srivastava, P.; Sharma, P.K.; Muheem, A.; Warsi, M.H. Magnetic nanoparticles: A review on stratagems of fabrication and its biomedical applications. *Recent Pat. Drug. Deliv. Formul.* **2017**, *11*, 101-113.
10. Mosayebi, J.; Kiyasatfar, M.; Laurent, S. Synthesis, functionalization, and design of magnetic nanoparticles for theranostic applications. *Adv. Healthc. Mater.* **2017**, *6*, 23.
11. Ito, A.; Kamihira, M. Tissue engineering using magnetite nanoparticles. *Prog. Mol. Biol. Transl. Sci.* **2011**, *104*, 355-395.
12. Masudi, A.; Harimisa, G.E.; Ghafar, N.A.; Jusoh, N.W.C. Magnetite-based catalysts for wastewater treatment. *Environ. Sci. Pollut. Res. Int.* **2020**, *27*, 4664-4682.
13. Ghaferah, H.A.I.; Abdel Majid, A.A.; Mohamed, G.El.; Ashraf, A.El.; Amnah, M.A.I.; Moamen, S.R. Efficient adsorption of Rhodamine B using a composite of Fe<sub>3</sub>O<sub>4</sub>@zif-8: Synthesis, characterization, modeling analysis, statistical physics and mechanism of interaction. *Bull. Chem. Soc. Ethiop.* **2023**, *37*, 211-229.
14. Farahbakhsh, J.; Vatanpour, V.; Ganjali, M.R.; Saeb, M.R. *21 - Magnetic Nanoparticles in Wastewater Treatment, Magnetic Nanoparticle-Based Hybrid Materials, Fundamentals and Applications*, Woodhead Publishing Series in Electronic and Optical Materials; **2021**, 547-589. <https://doi.org/10.1016/B978-0-12-823688-8.00036-3>.
15. Altaf, S.; Zafar, R.; Zaman, W.Q.; Ahmad, S.; Yaqoob, K.; Syed, A.; Khan, A.J.; Bilal, M.; Arshad, M. Removal of levofloxacin from aqueous solution by green synthesized magnetite (Fe<sub>3</sub>O<sub>4</sub>) nanoparticles using *Moringa olifera*: Kinetics and reaction mechanism analysis. *Ecotoxicol. Environ. Saf.* **2021**, *226*, 112826.
16. Shi, X.; Zhang, X.; Gao, W.; Zhang Y.; He, D. Removal of microplastics from water by magnetic nano-Fe<sub>3</sub>O<sub>4</sub>. *Sci. Total Environ.* **2022**, *802*, 149838.
17. Gupta, P.; Ramrakhiani, M. Influence of the particle size on the optical properties of CdSe nanoparticles. *Open Nanoscience J.* **2009**, *3*, 15-19.
18. Das, A.K.; Marwal A.; Verma R. Bio-reductive synthesis and characterization of plant protein coated magnetic nanoparticles. *nano. Hybrids* **2014**, *7*, 69-86.
19. Pervin, R.; Khan, K.A.; Khan, N.I.; Atique Ullah, A.K.M.; Zian Reza, S.M. *Green Synthesis of Magnetite (Fe<sub>3</sub>O<sub>4</sub>) Nanoparticles using Azadirachta indica Leaf Extract and Their Characterization in Advances in Medical Physics and Healthcare Engineering, Lecture Notes in Bioengineering*, Mukherjee, M.; Mandal, J.; Bhattacharyya, S.; Huck, C.; Biswas, S. (Eds.), Springer: Singapore; **2021**. [https://doi.org/10.1007/978-981-33-6915-3\\_9](https://doi.org/10.1007/978-981-33-6915-3_9).
20. Sabiu, A.; Sadik G.; Yuksel K.; Ibrahim M.; Bala A.; Mahmud, A. Simple method for the determination of band gap of a nanopowdered sample using Kubelka Munk theory. *J. Nigerian Association of Mathematical Physics* **2016**, *35*, 241-246.
21. Sujit, A.K.; Giang, T.P.; Duy, V.P.; Ranjit, A.P.; Chien-Chih, L.; Yan-Ruei, C.; Yung, L.; Yuan-Ron, M. Doping-free bandgap tunability in Fe<sub>2</sub>O<sub>3</sub> nanostructured films. *Nanoscale Adv.* **2021**, *3*, 5581.
22. Rahdar, A. Effect of 2-mercaptoethanol as capping agent on ZnS nanoparticles: structural and optical characterization. *J. Nanostruct. Chem.* **2013**, *3*, 10.
23. Link, S.; El-Sayed, M.A. Shape and size dependence of radiative, non-radiative and photothermal properties of gold nanocrystals. *Int. Rev. Phys. Chem.* **2010**, *19*, 409-453.
24. Yeshchenko, O.A.; Dmitruk, I.M.; Alexeenko, A.A.; Kotko, A.V.; Verdal, J.; Pinchuk, A.O. Size and temperature dependence of the surface plasmon resonance in silver nanoparticles. *Plasmonics* **2012**, *7*, 685-694.
25. Lasse, K.S.; Daniil, E.K.; Valeriy, S.G.; Alexander, E.E.; Sergey, P.P.; Sergey, V.K.; Hans, Å. *J. Phys. Chem. C* **2022**, *126*, 16804-16814.